Glycosylphosphatidylinositol-dependent secretory transport in *Trypanosoma brucei*

Mary Ann McDOWELL[1], Dawn M. RANSOM and James D. BANGS[2]

Department of Medical Microbiology and Immunology, University of Wisconsin-Madison Medical School, 1300 University Avenue, Madison, WI 53706, U.S.A.

We have investigated the role of glycosylphosphatidylinositol (GPI) anchors in forward secretory trafficking using African trypanosomes as a model system. Soluble GPI-minus forms of variant surface glycoprotein (VSG), in which the C-terminal GPI-addition peptide signal is deleted, are secreted from transformed procyclic trypanosomes with 5-fold reduced kinetics, relative to matched GPI-anchored constructs. Cell fractionation and immunofluorescence localization studies indicate that the GPI-minus VSG reporters accumulate in the endoplasmic reticulum (ER). This transport defect is specific, since overexpression of GPI-minus VSG has no effect on the rate of transport of a second soluble secretory reporter (BiPN) when co-expressed in the same cells. Two results suggest that delayed forward transport cannot be accounted for by failure to fold/assemble in the absence of a GPI anchor, thereby leading to prolonged association with ER quality-control machinery. First, no evidence was found for elevated association of GPI-minus VSG with the ER molecular chaperone, BiP. Secondly, newly synthesized GPI-minus VSG is dimerized efficiently, as judged by velocity-sedimentation analysis. GPI-dependent transport is not confined to the VSG reporters, because a similar dependence is found with another trypanosomal GPI-anchored protein, trans-sialidase. These findings suggest that GPI structures act in a positive manner to mediate efficient forward transport of some, and perhaps all, GPI-anchored proteins in the early secretory pathway of trypanosomes. Possible mechanisms for GPI-dependent transport are discussed with respect to current models of vesicular trafficking.

INTRODUCTION

Membrane glycoproteins that are attached to the lipid bilayer via glycosylphosphatidylinositol (GPI) anchors are ubiquitous in eukaryotes. Among the best studied of these proteins are the variant surface glycoprotein (VSG) of African trypanosomes [1], the T-cell marker Thy-1 [2,3] and placental alkaline phosphatase [4]. The basic mechanism of GPI synthesis and covalent attachment to nascent secretory polypeptides is conserved in all eukaryotic cells [5,6]. In a process that occurs immediately after translocation into the endoplasmic reticulum (ER), attachment is directed by a C-terminal hydrophobic GPI-attachment signal peptide (GPI-peptide), which is replaced in a transamidation reaction by a preformed GPI precursor. Although many proteins are known to possess GPI anchors, and much is known concerning the mechanism of attachment, the greater functional role(s) of this moiety, other than to attach proteins to membranes, has yet to be completely elucidated.

One process in which GPI anchors are clearly implicated is the post-Golgi targeting of apical membrane proteins in polarized epithelial systems; both endogenous and recombinant GPI-linked proteins are distributed apically in such cells (reviewed in [7]). Furthermore, replacement of the transmembrane and cytoplasmic domains of basolateral membrane proteins with recombinant GPI-peptides results in targeting to the apical membrane [8,9]. These findings indicate that GPI anchors can function as specific targeting signals, at least in polarized epithelial cells.

Other results suggest that GPI anchors may also function in the transport of proteins from the ER. Disruption of GPI attachment, either in cell lines that are deficient in GPI precursor synthesis or by mutation of GPI-peptides, can result in the retention of mammalian GPI-anchored proteins in the ER [10–12]. Typically, in such cases, the GPI-peptide remains uncleaved and these proteins are ultimately degraded. Similarly, when GPI synthesis is blocked by inositol starvation in auxotrophic yeast, the most abundant GPI-anchored protein, Gas1p, fails to exit the ER [13]. The GPI-peptide remains uncleaved and reversal of the block with exogenous inositol allows renewed GPI synthesis/attachment and exit from the ER. These findings suggest that GPI anchors may function in forward transport in the early secretory pathway, but, since in each of the cases cited the GPI-peptide remains uncleaved, it is not possible to tell whether it is the absence of a GPI anchor or the presence of the GPI-peptide that leads to retention. However, conversion of the E1 membrane glycoprotein of Rubella virus to a GPI-anchored form over-rides a pre-Golgi localization signal present in the E1 lumenal domain, resulting in transport to the cell surface [14]. This finding provides evidence of a more direct nature that GPI structures can mediate forward transport in a positive manner.

Our laboratory has exploited African trypanosomes, the organisms in which GPI anchors were first characterized [1], to investigate the role of this moiety in intracellular trafficking [15]. Trypanosomes have a life cycle that alternates between an insect vector, the tsetse fly, and the bloodstream of mammalian hosts. Each stage expresses a distinct GPI-anchored cell-surface coat protein, homodimeric VSG in the bloodstream stage, and the monomeric procyclic acidic repetitive protein (PARP; also called procyclin) in the procyclic insect stage [16,17]. Using a stable transformation system, we have shown previously that recombinant VSG can be expressed in procyclic trypanosomes. This

Abbreviations used: ER, endoplasmic reticulum; GPI, glycosylphosphatidylinositol; GPI-peptide, GPI-attachment signal peptide; HBS, Hepes buffered saline; NGS, normal goat serum; PARP, procyclic acidic repetitive protein; PIC, protease inhibitor cocktail; TS, trans-sialidase; VSG, variant surface glycoprotein; VSGΔgpi, GPI-peptide-deleted VSG.

[1] Present address: Laboratory of Parasitic Diseases, National Institutes of Health/NIAID, Building 4, Room 126, Bethesda, MD 20892, U.S.A.

[2] To whom correspondence should be addressed (e-mail bangs@macc.wisc.edu).

VSG is GPI-anchored, dimerized, exported to the cell surface efficiently ($t_{\frac{1}{2}} \approx 1$ h) and then released by the action of an endogenous zinc metalloendoprotease [15]. In contrast, recombinant forms of VSG, truncated at the site of GPI addition to yield GPI-peptide-deleted VSG (VSGΔgpi), are exported in a soluble manner with greatly reduced kinetics ($t_{\frac{1}{2}} \approx 5$ h). Fusion of the PARP GPI-peptide to truncated VSG restores both GPI attachment and rapid transport. These findings clearly imply a role for the GPI anchor in timely forward export of VSG. Two basic models were proposed to account for GPI-dependent transport of VSG. The first holds that, in the absence of a GPI anchor, soluble VSGΔgpi is unable to fold/dimerize and is retained in the ER by resident quality-control machinery [18]. In the alternative model, VSG assembly is unimpeded, but some property essential for transport and imparted by the GPI anchor is missing.

In this study, we investigate the transport defect of VSGΔgpi in an attempt to discriminate between these models. We first demonstrate that cell-associated VSGΔgpi is located in the ER, and that the overexpression of this protein has no global effects on the transport of other soluble secretory cargo. Secondly, we demonstrate that newly synthesized VSG is efficiently folded and dimerized in the absence of a GPI anchor. These results indicate that a failure to assemble cannot account for the reduced transport kinetics of VSGΔgpi, and that the GPI anchor is necessary for transport of these proteins. Finally, we extend our observation of GPI-dependent forward transport to a second GPI-anchored protein, the trans-sialidase (TS) of *Trypanosoma cruzi*. Thus it appears that GPI-dependent transport is a common feature of GPI-anchored proteins in trypanosomatid protozoa. These findings are interpreted in the light of current models of vesicular secretory trafficking.

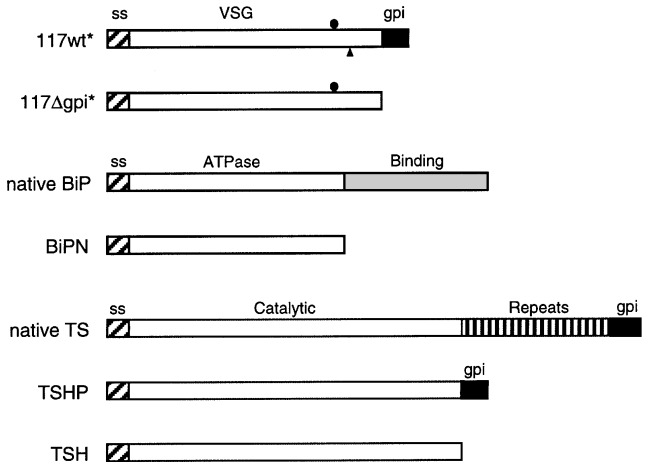

Figure 1 Diagram of secretory reporters

Diagrammatic representations (approx. to scale) of VSG, BiP and TS-derived secretory reporters are shown. The schematic domain structures of native BiP and TS are shown for comparison. Domain regions are: N-terminal signal sequences (ss; hatched boxes); VSG-coding region, BiP ATPase domain and TS catalytic domains (open boxes); BiP peptide-binding domain (grey box); TS repeat region (vertical stripes); and GPI-peptide sequences (gpi; black boxes). The approximate positions of the 117wt C-terminal proteolytic cleavage site (filled triangle) and the single VSG 117 N-glycosylation site (filled circle) are indicated. Asterisks indicate where analogous VSG 221wt and 221Δgpi reporters were also used. Sequence/domain information was from [21,22,24,48].

EXPERIMENTAL

Maintenance and manipulation of trypanosomes

All experiments involving expression of single recombinant reporters were performed with uncloned, stably transfected *T. brucei* strain 427 procyclic cell lines. In experiments requiring double reporter expression, a cell line expressing the 117Δgpi reporter (hygromycin-resistant) was cloned by limiting dilution and the clonal line was used for transfection with a BiPN reporter construct under neomycin selection. The resultant uncloned double-transfected cell line was used for pulse–chase radiolabelling experiments. The maintenance, transformation and radiolabelling of procyclic cell lines have been described previously [19]. Cell-surface biotinylation and the release of biotinylated reporters were performed exactly as described previously [15]. The zinc-specific chelator, bathophenathroline (Sigma, St. Louis, MO, U.S.A.), was used as an inhibitor of reporter release.

Transport of reporters to the cell surface was directly measured in a trypsin sensitivity assay (all steps at 0 °C). Aliquots of cells from pulse–chase experiments (1.0 ml, 10^7 cells) were washed once in Hepes buffered saline (HBS) [50 mM Hepes/KOH (pH 7.5)/50 mM NaCl/5 mM KCl/70 mM glucose/5.5 mM proline/1 mM $CaCl_2$] and resuspended in 100 μl of trypsin (0.5 mg/ml in HBS, tosyl-lysylchloromethane-treated, Type XIII, 11 700 units/mg; Sigma). After incubation (20 min), 400 μl of chicken egg-white trypsin inhibitor was added directly (2.0 mg/ml in HBS, Type III-O; Sigma) for a further 5 min. Cells were collected by centrifugation and then washed with HBS (without $CaCl_2$) containing 1 mg/ml ovalbumin and 1 mM PMSF. Cells were solubilized for immunoprecipitation (see below) in the presence of protease inhibitor cocktail (PIC; where 1 × PIC contains 4 μg/ml each of leupeptin, antipain, pepstatin and chymostatin), ovalbumin (1 mg/ml) and trypsin inhibitor (0.1 mg/ml).

Immunoprotocols, antibodies and electrophoresis

Immunoprecipitation, immunoblotting, electrophoresis and fluorography have been reported previously [15]. All lysates and gradient fractions were supplemented with 1 × PIC before immunoprecipitation. Except for gradient fractions (see below), all immunoprecipitations were performed in RIPA buffer [20]. Rabbit anti-(*T. brucei* BiP), anti-(VSG 117) and anti-(VSG 221) antibodies used in this study have also been described previously [15,21]. Mouse antiserum raised against purified VSG 117 was generated in Swiss Webster mice using the RIBI adjuvant system (RIBI ImmunoChem Research Inc., Hamilton, MT, U.S.A.). Rabbit anti-(*T. cruzi* TS) and mouse anti-(*T. cruzi* BiP) sera were generously given by Dr. Sergio Schenkman (Universidade Federal De Sao Paulo, Sao Paulo, Brazil) and Dr. David Engman (Northwestern University, Chicago, IL, U.S.A.) respectively. Rabbit antiserum against *T. brucei* hsp70 (gene 4) was prepared by Todd Kowalski (University of Wisconsin, WI, U.S.A.).

Construction of reporter genes

Diagrams of all reporter genes are shown in Figure 1. A hygromycin phosphotransferase gene cassette, with flanking *Asc*I and *Pac*I sites (generously given by Dr. Ian Manger, Stanford University, Stanford, CA, U.S.A.), was substituted for the neomycin cassette in the stable expression vector, pXS2 [19]. Construction of the VSG 117, VSG 221 and BiPN reporter genes used in this work has been described previously [15,19]. TS reporters were generated by PCR, and introduced into pXS2 in a similar manner. Briefly, the region encoding the *T. cruzi* TS catalytic domain (codons 1–667) [22] was amplified (primers

JB66/JB67) from the plasmid p154SII (generously given by Dr. Dan Eichinger, New York University, New York, NY, U.S.A.) and subcloned such that the C-terminus was fused to either the HA9 epitope alone (TSH) or the HA9 epitope followed by the PARP GPI-peptide (TSHP) (Figure 1). The HA9 epitope [23] was included in these constructs solely as a cloning convenience; we have previously shown that this has no effect on trafficking of either the soluble or GPI-anchored secretory reporters in *T. brucei* [15,19].

The following synthetic deoxyoligonucleotides were used for PCR. Sequences complementary to the target template are in upper case; added sequences are lower case. Restriction sites are underlined; all sequences are 5′ → 3′: JB66, cagcagatcgatATGGGGAAAACAGTC, 5′-sense primer for TS (codons 1–5) with *Cla*I site; JB67, acgacggctagcGCTGCCCATGTGTGC, 3′-antisense primer for TS (codons 663–667) with *Nhe*I site.

Velocity-sedimentation analysis

Procyclic cells (5×10^8) expressing various reporters were pulse-labelled with [^{35}S]Met/[^{35}S]Cys (Expre^{35}S^{35}S, Dupont NEN, Boston, MA, U.S.A.) for 15 min (10^8 cells/ml; 200 μCi/ml), washed twice with PBS and then extracted (5 min, 22 °C) in 1.0 ml of TEN buffer [50 mM Tris/HCl (pH 7.5)/150 mM NaCl/5 mM EDTA] containing 1 % (v/v) Nonidet P40. Insoluble material was removed by centrifugation (30 min, 100000 ***g***) using a Beckman 70.1Ti rotor). Loaded samples (0.5 ml) of either spent culture media or whole cell Nonidet P40 extracts were centrifuged on 11-ml linear 10–20 % (w/w) sucrose gradients in 50 mM Tris/HCl, pH 7.5, for 24 h [200000 ***g***, 25 °C] using a Beckman SW41.Ti rotor. For cell extracts, 0.1 % (w/v) Nonidet P40 was also included in the gradient. Molecular-mass standards included internally for extracts, or run on parallel gradients for culture supernatants, were as follows (250 μg of each): bovine γ-globulin (Sigma), 170 kDa; BSA (Sigma), 67 kDa; and carbonic anhydrase (Sigma), 31 kDa. Following centrifugation, ≈ 640 μl fractions were collected from the top and VSG was detected in each fraction by either immunoblotting (10–25 μl samples) or immunoprecipitation (directly from 300–500 μl). Samples of each fraction (25 μl) were separated by SDS/PAGE, and standards were revealed by Coomassie Blue staining.

Immunofluorescence

Washed exponential-phase procyclic trypanosomes (400 μl, 10^7/ml) in PBS supplemented with 1 mg/ml glucose (PBSG) were spread on slides, allowed to settle until the proper density was reached (≈ 5 min), and then non-adherent cells were washed away with PBSG. Slides were air-dried and then fixed sequentially with methanol and then acetone at −20 °C (3 min each). After drying, silicone rubber 2 × 5-well forms were clamped on and staining was performed in individual wells. Wells were blocked (1 h) with PBS/10 % (v/v) normal goat serum (NGS) and then treated (1 h) with primary antibodies [50 μl, 1:200 in PBS/10 % (v/v) NGS]. Wells were washed four times with PBS/1 % (v/v) NGS and then treated (1 h) with fluorescein- or rhodamine-conjugated secondary antibodies [50 μl, 1:100 (v/v) in PBS/10 % (v/v) NGS, goat anti-(mouse IgG) and anti-(rabbit IgG) antibody, Kirkegaard and Perry Laboratories Inc., Gaithersburg, MD, U.S.A.]. Hoechst 33258 dye (0.1 μg/ml) was included in the secondary antibody to stain nuclear and kinetoplast DNA. Wells were again washed four times with PBS/1 % (v/v) NGS, and slides were mounted with PBS/50 % (v/v) glycerol containing *m*-phenylenediamine (Sigma) as anti-fade. Specific staining was viewed by epifluorescence on a Zeiss Axioskop (Carl Zeiss Inc., Thornwood, NY, U.S.A.) at 100 × magnification. Appropriate emission/excitation filters were used for fluorescein and rhodamine. Images were captured using a digital cooled CCD MicroMax camera equipped with a 1317 × 1035 pixel array (Princeton Instruments, Trenton, NJ, U.S.A.) and processed using IPLab Spectrum imaging software (Signal Analytics Corp., Vienna, VA, U.S.A.).

RESULTS

Subcellular localization of GPI-minus VSG

The export of at least one trypanosomal cell-surface protein, VSG, is critically dependent on the presence of a GPI anchor [15,19]. Recombinant VSG reporters lacking the GPI-peptide sequence specifying GPI addition (e.g. 117Δgpi, Figure 1) are secreted in a soluble manner, but with a substantial reduction in export kinetics ($t_{\frac{1}{2}} \approx 5$ h) relative to GPI-anchored controls ($t_{\frac{1}{2}} \approx 1$ h). No intracellular degradation of GPI-minus reporters occurs; consequently, large amounts of VSG polypeptide accumulate within these cells, relative to GPI-anchored controls (see also Figure 5). Comparative immunoblot analysis indicates that the level of cell-associated VSG in the 117Δgpi procyclic cell line is approx. one-twentieth of that in bloodstream trypanosomes naturally expressing the same VSG (Figure 2A; compare lanes 3 and 5). A single bloodstream trypanosome contains ≈ 10^7 molecules of VSG [16], therefore transformed procyclics have ≈ 5×10^5 reporter molecules, a level approaching the total mass of the major endogenous procyclic surface protein, PARP [24].

Cell-fractionation experiments with VSGΔgpi-expressing cell lines indicate that the cell-associated VSG is a soluble lumenal component of crude microsomal vesicles (results not shown). To determine more precisely the intracellular location of VSGΔgpi, we performed double indirect immunofluorescence assays on the 117Δgpi and 221Δgpi procyclic cell lines. Fixed permeabilized cells were stained simultaneously with antibodies against BiP and the appropriate VSG (Figure 3). The pattern of staining seen

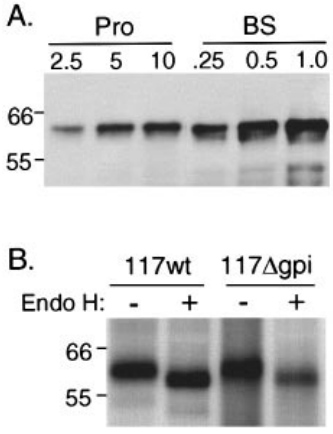

Figure 2 Expression and N-glycosylation of VSG 117Δgpi

(**A**) Samples of total cell extracts containing increasing cell equivalents of a procyclic cell line expressing recombinant 117Δgpi VSG (Pro) or bloodstream trypanosomes naturally expressing VSG 117 (BS) were analysed by immunoblotting with anti-(VSG 117) serum. Cell equivalents per lane ($\times 10^{-5}$) are indicated. (**B**) Procyclic cell lines expressing 117wt or 117Δgpi reporters were radiolabelled with [^{35}S]Met/[^{35}S]Cys for 4 h and VSG polypeptides were immunoprecipitated specifically from cell extracts. Immunoprecipitates were mock-treated (−) or endoglycosidase-H-treated (+) as described in [15], and analysed by SDS/PAGE/fluorography. A scan of a 3-day exposure is presented. Scales refer to molecular mass in kDa.

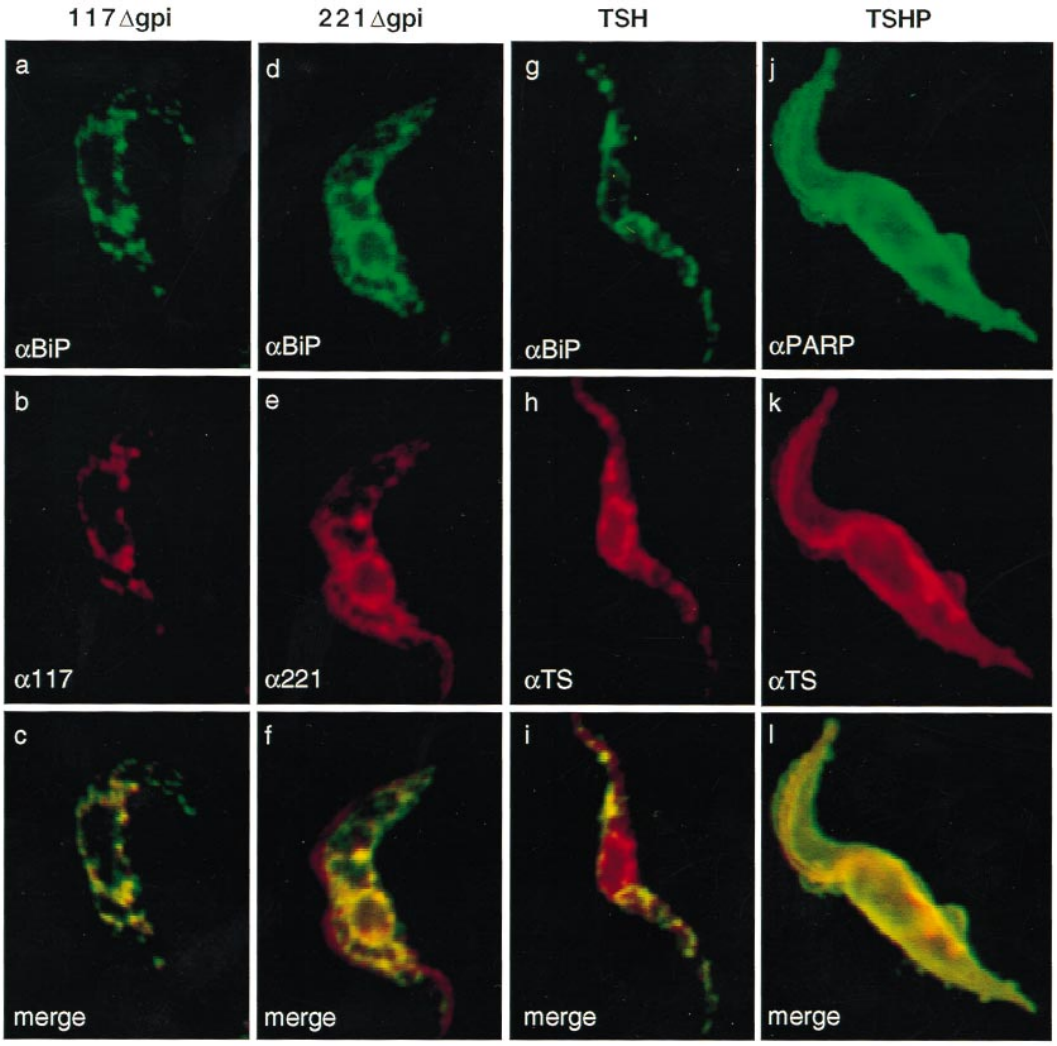

Figure 3 Immunolocalization of VSGΔgpi

Fixed and permeabilized procyclic cells expressing various reporters were treated as follows: 117Δgpi cells (**a**–**c**) with rabbit anti-BiP and mouse anti-(VSG 117); 221Δgpi cells (**d**–**f**) with mouse anti-BiP and rabbit anti-(VSG 221); TSH cells (**g**–**i**) with mouse anti-BiP and rabbit anti-TS; and TSHP cells (**j**–**l**) with monoclonal anti-PARP and rabbit anti-TS. Specific immunofluorescent staining was detected after treatment with fluorescein- and rhodamine-conjugated secondary antibodies, and is presented in green pseudocolour (BiP: **a**, **d**, **g**; PARP: **j**) and red pseudocolour (VSG: **b** and **e**; TS: **h** and **k**). Digital merging of matched BiP and VSG images (**c** and **f**), BiP and TS images (**i**) and PARP and TS images (**l**) result in yellow pseudocolour in regions of co-localization. Specific cell lines are identified at the top of each column.

with anti-BiP (Figures 3a and 3d) is characteristic of the ER morphology in trypanosomes [21]. The pattern of staining seen with anti-(VSG 117) (Figure 3b) and anti-(VSG 221) (Figure 3e) resembles very closely the distribution of BiP seen within the same cells. This is best seen in the digitally merged images (Figures 3c and 3f), where the almost exact co-localization of BiP and VSG reporters results in predominantly yellow pseudocolour. No staining was observed with either normal sera in transformed cells or anti-VSG antibodies in untransformed cells (results not shown). We conclude that the bulk of the cell-associated VSGΔgpi reporters are located in the ER, the initial compartment of the secretory pathway.

Overexpression of VSGΔgpi has no global effects

Our results suggest that the rate-limiting step in transport of VSGΔgpi is exit from the ER. A trivial explanation for this finding is that accumulation of GPI-minus reporters leads to a general depression of forward transport from the ER. To investigate this possibility, we introduced the gene for a second soluble secretory reporter (BiPN, comprising the N-terminal ATPase domain of trypanosomal BiP; see Figure 1) into a clonal cell line expressing 117Δgpi VSG. Secretion of the co-expressed reporters was then assessed in pulse–chase experiments (Figure 4) as the time-dependent disappearance from cells (Figure 4, lanes 1–6) and consequent appearance in the medium (Figure 4, lanes 7–12). The 117Δgpi reporter is exported from cells slowly over a 24-h chase period (Figure 4A), consistent with the kinetics defined previously for this reporter ($t_{\frac{1}{2}} \approx 5$ h) when expressed alone [15]. Simultaneously, BiPN is quantitatively exported within 4 h (Figure 4B), again consistent with previously defined kinetics ($t_{\frac{1}{2}} \approx 1$ h; [19]). Thus accumulation of 117Δgpi polypeptide in the ER does not affect the efficient transport of an independent soluble secretory reporter. We conclude that there is

no apparent global effect on transport, and that the defect is specific to the GPI-minus VSG reporters.

Glycosylation and assembly of GPI-minus VSG

The VSG117 reporters have a single N-glycosylation site (Figure 1) and we wished to determine if a failure to utilize this site could account for reduced transport of the GPI-minus reporters. Metabolically radiolabelled VSG polypeptides were immunoprecipitated from the 117wt and 117Δgpi cell lines and treated with endoglycosidase H (Figure 2B). In each case, treatment increases the electrophoretic mobility of the reporters by an amount consistent with the removal of one high-mannose oligosaccharide, indicating that the single N-glycosylation site in these reporters is occupied. Thus a lack of proper glycosylation cannot account for the decreased transport of GPI-minus VSG.

Another hypothesis that may account for the failure of VSGΔgpi to exit the ER is that newly synthesized reporter fails to fold and/or homodimerize efficiently in the absence of a GPI anchor. Such unfolded VSG polypeptides might then be retained in the ER by interaction with resident molecular chaperones in a process referred to as 'quality control' [18]. The only ER molecular chaperone currently characterized in trypanosomes is the ER heat-shock protein (hsp70) homologue, BiP [21]. To search for an elevated association with endogenous BiP, procyclic cell lines expressing either wild-type or GPI-minus forms of VSG 117 and VSG 221 reporters were radiolabelled metabolically, followed by immunoprecipitation with specific anti-VSG or anti-BiP antibodies (Figure 5). As is typical for these matched reporter pairs [15], there is significantly more cell-associated GPI-minus VSG relative to the wild-type reporters (Figure 5; compare lanes 1 and 2, and 5 and 6 respectively), the latter being shed continuously from the cell surface by an endogenous metalloprotease [15]. Despite the elevation of cell-associated VSGΔgpi, which we have shown is located primarily in the ER (see Figure 3), there are only minor increases in the amount of BiP-associated VSG polypeptides (Figure 5; compare lanes 4 and 3, and 8 and 7 respectively). It should be noted that a similar assay readily detects BiP-associated native VSG in bloodstream trypanosomes [19]; thus an interaction of unfolded polypeptide with the one ER molecular chaperone for which reagents are currently available cannot account for the elevated ER accumulation of the VSGΔgpi reporters. We cannot exclude the possibility that these proteins are retained by association with other, as yet uncharacterized, trypanosomal secretory molecular chaperones, e.g. calnexin or grp94.

We then wished to assess directly the state of folding/assembly of cell-associated VSGΔgpi. Assuming that dimerization cannot occur without proper folding, we determined the oligomeric state of both secreted and cell-associated Δgpi reporters by velocity sedimentation (Figure 6). Immunoblot analyses of fractionated culture supernatants (Figures 6A and 6C) indicated that the secreted forms of both GPI-minus reporters sediment as dimers. Thus these reporters are exported as dimers, and do not simply leak from cells in an unfolded form. To analyse cell-associated GPI-minus reporters, detergent extracts prepared from cells that had been radiolabelled for 15 min were fractionated in the same manner. Following velocity sedimentation, fractions were subjected to immunoblotting and immunoprecipitation to determine the oligomeric nature of both steady-state and newly synthesized GPI-minus reporters respectively. In each case, steady-state cell-associated VSGΔgpi polypeptides sedimented as dimers (results not shown), confirming that folding occurs before secretion. More importantly, newly synthesized GPI-minus reporters also sedimented as dimers (Figures 6B and 6D). Thus even at a time

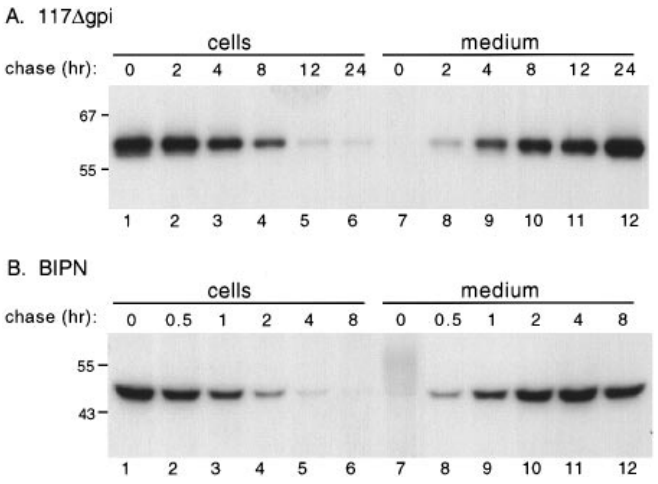

Figure 4 Effect of VSGΔgpi overexpression

A procyclic cell line co-expressing the soluble BiPN and 117Δgpi reporters was pulse-labelled for 15 min with [^{35}S]Met/[^{35}S]Cys and then chased for 24 h. At the indicated times, samples were taken and the presence of radiolabelled polypeptides in cell and medium fractions was analysed by specific immunoprecipitation with either (**A**) anti-(VSG 117) or (**B**) anti-BiP antibodies. Immunoprecipitates were fractionated by SDS/PAGE (12% gels); scans of typical fluorographs (2-day exposures) are presented. All lanes contain 5×10^6 cell equivalents. Scale refers to molecular mass in kDa.

point immediately following synthesis, when the presence of unfolded reporter might be expected, all detectable VSG is assembled into dimers. We conclude that a failure to fold/assemble in the absence of a GPI anchor cannot account for the failure of these reporters to be exported in a timely manner.

GPI-dependent transport of TS

Our results suggest that, at least for VSG, timely transport is dependent on the presence of a GPI anchor. To determine

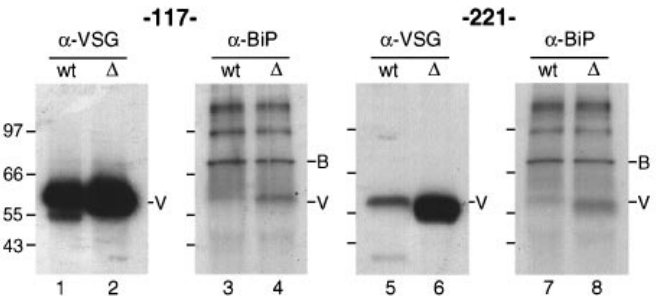

Figure 5 BiP-associated VSGΔgpi is not elevated

Procyclic cell lines expressing either full-length wild-type (wt; lanes 1, 3, 5 and 7) or truncated Δgpi (Δ; lanes 2, 4, 6 and 8) VSG reporters (VSG 117, lanes 1–4; VSG 221, lanes 5–8) were radiolabelled with [^{35}S]Met/[^{35}S]Cys for 4 h and polypeptides were specifically immunoprecipitated from cell extracts with either anti-(VSG 117) (lanes 1 and 2), anti-(VSG 221) (lanes 5 and 6) or anti-BiP (lanes 3, 4, 7 and 8) antibodies. Immunoprecipitates were analysed by SDS/PAGE fluorography. All lanes show 5×10^6 cell equivalents. All panels are from a single scan of an 8-h exposure from the same gel. This exposure was selected to allow direct comparison of the BiP and VSG signals; hence the increased level of 117Δgpi (lane 2) relative to 117wt (lane 1) is less apparent. The positions of VSG reporters (V) and endogenous BiP (B) are indicated. The scale refers to molecular mass in kDa. The high-molecular-mass bands seen in the anti-BiP immunoprecipitations are uncharacterized polypeptides that associate transiently with BiP in pulse–chase experiments [19].

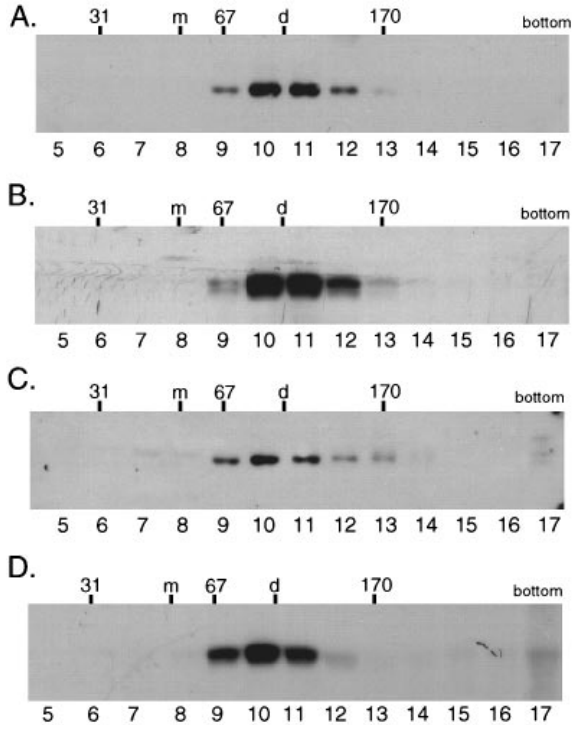

Figure 6 Velocity-sedimentation analysis of VSG reporters

Samples were subjected to velocity-sedimentation analysis on sucrose gradients, and fractions were taken from the top. Secreted VSG in gradient fractions of stationary-phase culture supernatants from 117Δgpi (**A**) and 221Δgpi (**C**) cells were detected by immunoblot with anti-VSG antibodies. Radiolabelled VSGΔgpi in gradient fractions of cell extracts from 15-min pulse-labelled 117Δgpi (**B**) and 221Δgpi (**D**) cell lines was detected by immunoprecipitation and SDS/PAGE/fluorography. Fraction numbers are indicated. The sedimentation positions of molecular-mass standards (bovine γ-globulin, 170 kDa; BSA, 67 kDa; and carbonic anhydrase, 31 kDa) were determined by Coomassie Blue staining of SDS/PAGE gels, and are indicated in kDa over peak fractions or between fractions of approx. equal intensity. The predicted positions of dimeric (d) and monomeric VSG (m) were interpolated from graphs of standard mass versus peak fraction, and were confirmed for purified bloodstream soluble VSG on separate native and denaturing gradients (results not shown).

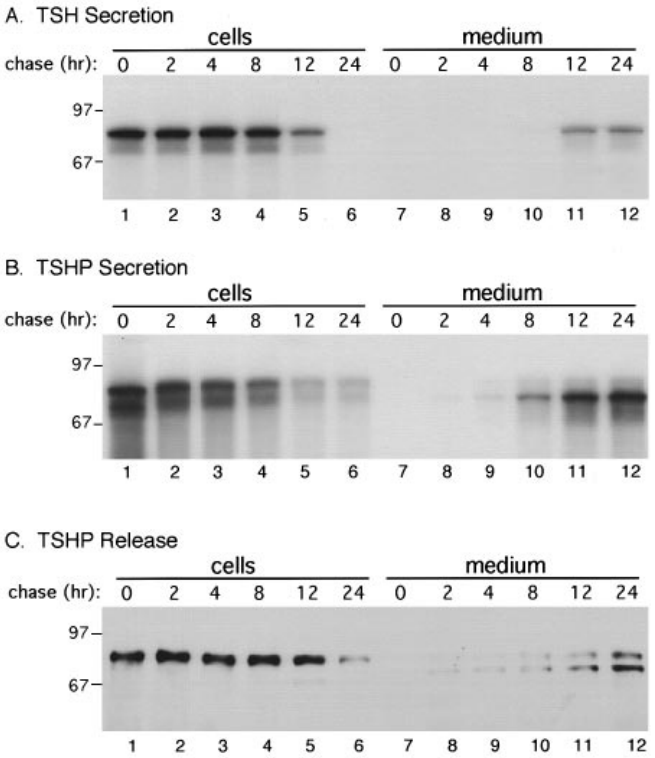

Figure 7 Export of TS reporters

The mode of secretion of GPI-minus (TSH) and GPI-plus (TSHP) TS reporters was investigated. TSH (**A**) and TSHP (**B**) cell lines were pulse-labelled for 15 min and then chased. The presence of labelled reporters in cells and medium fractions was assayed by immunoprecipitation, as described in Figure 4. (**C**) TSHP-expressing cells were surface-biotinylated and placed in culture. At subsequent time points, samples were separated into cell and medium fractions, and TSHP polypeptides were immunoprecipitiated and fractionated by SDS/PAGE (10% gels). After electrophoretic transfer to membranes, biotinyl-TSHP was detected by chemiluminescence using avidin–horseradish peroxidase.

whether this finding is specific for VSGs, or whether it is a generalized phenomenon for other GPI-anchored molecules, we expressed modified TS genes from the related trypanosomatid, *T. cruzi*. The wild-type TS gene [22] encodes a GPI-anchored protein with an N-terminal catalytic domain of $\approx$ 73 kDa and a C-terminal repeat domain of $\approx$ 35 kDa followed by a GPI-peptide sequence (see Figure 1). To simplify our analysis, we constructed matched reporters composed of the catalytic domain alone (TSH) and the catalytic domain fused to the GPI peptide of PARP (TSHP). We have previously demonstrated [15] that this PARP sequence is sufficient to reconstitute GPI anchoring and transport of VSGΔgpi reporters. Culture media derived from stably transformed procyclic cell lines expressing these reporters contain sialidase activity that is detectable above the background of endogenous *T. brucei* sialidase activity in medium derived from untransformed cells (measured by hydrolysis of methylumbelliferyl-*N*-acetylneuraminic acid; results not shown), suggesting that, like the VSG reporters, both forms of TS are released from cells.

Double immunofluorescence was utilized to evaluate the specific cellular localization of each TS reporter. The TSHP reporter gave a diffuse staining pattern that was identical with the distribution of the major procyclic cell-surface protein PARP (Figure 3, j–k), indicating a cell-surface localization. A similar pattern of cell-surface expression was seen with the GPI-anchored VSGwt reporters (results not shown). The pattern of staining seen with the GPI-minus TSH reporter, aside from a consistently elevated perinuclear accumulation, is essentially the same as that seen for the VSGΔgpi reporters, i.e. a prominent co-localization with the ER marker BiP (Figure 3, g–i). No staining of untransformed trypanosomes with anti-TS antibody was detected (results not shown). These results suggest that, as with the analogous VSG reporters, efficient transport of the TS reporters from the ER is dependent on the presence of a GPI-peptide sequence and, presumably, a GPI anchor.

To investigate the transport of these reporters, standard pulse–chase experiments were performed. Each cell line was labelled for 15 min and then, during a 24-h chase period, levels of released, cell-associated TS were evaluated by immunoprecipitation. Consistent with its predominant intracellular localization, GPI-minus TSH was slowly secreted during the chase (Figure 7A). However, the recovery of exported reporter was not quantitative (Figure 7; compare lanes 1 and 12), suggesting that some intracellular degradation may have been occurring. Although the $t_{\frac{1}{2}}$ of TSH transport could not be accurately quantified, owing to this degradation, it is clearly in excess of 8 h, slower even than GPI-minus VSG ($t_{\frac{1}{2}} \approx 5$ h). In comparable pulse–chase

experiments, the GPI-anchored TSHP reporter is initially found as a cell-associated doublet composed of a major high-molecular-mass form and a less abundant smaller species (Figure 7B, lane 1; see also Figure 8A, lane 1). The difference between these two species is not certain; however, since only the major form is found on the cell surface (see Figure 7C), we have focused our analysis on this species. Consistent with the presence of sialidase activity in culture medium, TSHP disappears from cells in a time-dependent manner (Figure 7B, lanes 1–6) and appears in the medium as a truncated form (Figure 7B, lanes 7–12). The truncation of TSHP suggests that shedding occurs by the same process as the release of GPI-anchored VSGwt reporters, i.e. cleavage proximal to the C-terminus by an endogenous cell-surface metalloprotease [15]. However, unlike the VSGwt reporters, which are quantitatively released in 4 h, TSHP shedding is greatly delayed, requiring 12–24 h to approach completion, and thereby leaving the issue of GPI-dependent transport in doubt.

As release is presumed to be a two-step process, first involving transport to the cell surface and then cleavage, two possibilities might explain the slow kinetics of TSHP shedding. If TSHP is a good substrate for the surface metalloprotease, then the rate-limiting step would be transport to the cell surface. Alternatively, cleavage might be rate-limiting, in which case the rate of transport could vary widely, providing that it is faster than the rate of cleavage. Our immunolocalization results are consistent with the latter alternative, but to confirm this we measured the rate of shedding of the steady-state pool of surface TSHP using a cell-surface biotinylation assay designed originally to follow release of VSGwt reporters [15]. As can be seen in Figure 7(C), the level of cell-associated biotinyl-TSHP decreased slowly during the 24-h incubation (lanes 1–6), concomitant with the appearance of predominantly truncated reporter in the medium (lanes 7–12). A small amount of TSHP was also shed slowly without apparent cleavage; this has not been further investigated. Release of the truncated form of TSHP, but not the full-length form, was reduced substantially by bathophenathroline (results not shown), an inhibitor of the metalloprotease [15]. These findings suggest that most cell-associated TSHP is released by proteolysis, and that cleavage is the rate-limiting step in secretion of biosynthetically labelled reporter.

To determine the actual rate of TSHP transport, cells were pulse–chase radiolabelled, and at various chase times susceptibility of cell-associated TSHP to digestion by exogenously added trypsin was assessed (Figure 8A). At the beginning of the chase period, essentially all of the labelled reporter was resistant to digestion, and was therefore intracellular (Figure 8; compare lanes 1 and 2). Subsequently, labelled TSHP became increasingly susceptible to trypsin (lanes 3–5) until, at 4 h, all the reporter was digested (compare lanes 6 and 7), indicating complete transport to the cell surface. As a control for assessment of cell integrity, the trypsin sensitivity of an endogenous cytoplasmic marker, hsp70 (Figure 8, lanes 9–12), was also determined by specific immunoprecipitation. hsp70 remained substantially resistant to digestion during the chase period, confirming that the trypsin assay faithfully reflects arrival of the reporter at the cell surface. Densitometric analysis indicated the rate of TSHP transport to be $t_{\frac{1}{2}} \approx 1.2$ h, i.e. at least 7-fold faster than the matched GPI-minus TSH reporter. Thus, like VSG, rapid transport of TS to the cell surface is critically dependent on GPI anchoring.

Finally, we have also assessed directly the transport of 117wt VSG using the trypsin assay (Figure 8B); this rate had previously been estimated indirectly by following release after arrival at the cell surface due to cleavage by the endogenous metalloprotease [15]. This constitutive release is evident by comparing the control

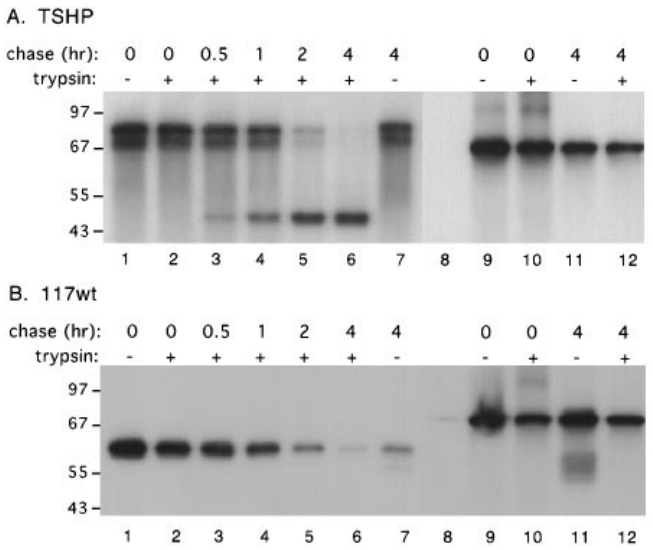

Figure 8 Kinetics of GPI-anchored reporter transport

Cell lines expressing TSHP (**A**) or 117wt (**B**) reporters were pulse-labelled for 15 min and then chased. At the indicated times, samples of cells were treated with trypsin (+) or mock-treated (−), and then the levels of cell-associated GPI-anchored reporter (lanes 1–7) or endogenous hsp70 (lanes 9–12) were assayed by immunoprecipitation, as in Figure 4. (**A**) Scans of 3-day (lanes 1–7) and 1-day (lanes 9–12) exposures are shown; all lanes are from the same gel. (**B**) A scan of a single 1-day exposure is shown. In all lanes, chase times and the positions of molecular-mass markers (kDa) are indicated. Densitometric analyses of duplicate scanned fluorographs were performed with the public domain NIH Image programme (http://rsb.info.nih.gov/nih-image/).

levels of cell-associated VSG at the beginning with those at the end of the chase period (Figure 8B, lanes 1 and 7). In this experiment, time-dependent loss of VSG (Figure 8B, lanes 2–6) represents the sum of release by both the endogenous protease and subsequent trypsin treatment. This combined loss provides a direct measure of arrival at the cell surface, and densitometric analysis indicates the rate of transport to be almost identical with that of TSHP ($t_{\frac{1}{2}} \approx 1.2$ h), confirming the original estimate for 117wt.

DISCUSSION

Recombinant reporter proteins for which GPI anchoring is prohibited by deletion of the C-terminal GPI-peptide sequence are exported from procyclic trypanosomes with greatly reduced kinetics relative to matched GPI-anchored constructs, and consequently accumulate in the ER. In other studies, where disruption of GPI attachment leads to ER retention, mislocalization has been attributed to the presence of an uncleaved GPI-peptide sequence, resulting in either aggregation or prolonged association with the GPI transamidase that catalyses attachment [10,12,13,25–27]. In contrast, our GPI-minus reporters are freely soluble, allowing a direct assessment of the function of GPI structures in exit from the ER. Others have also reported that analogous GPI-minus constructs are secreted from cell types as varied as polarized mammalian epithelial cells, yeast and *Dictyostelium* [8,9,28,29]; however, to our knowledge, none of these studies have determined actual rates of export. Since our results cannot be attributed to either a failure to N-glycosylate GPI-minus reporters or a global depression of secretion, we conclude that the reporters used here are critically dependent on the presence of a GPI anchor for timely forward transport.

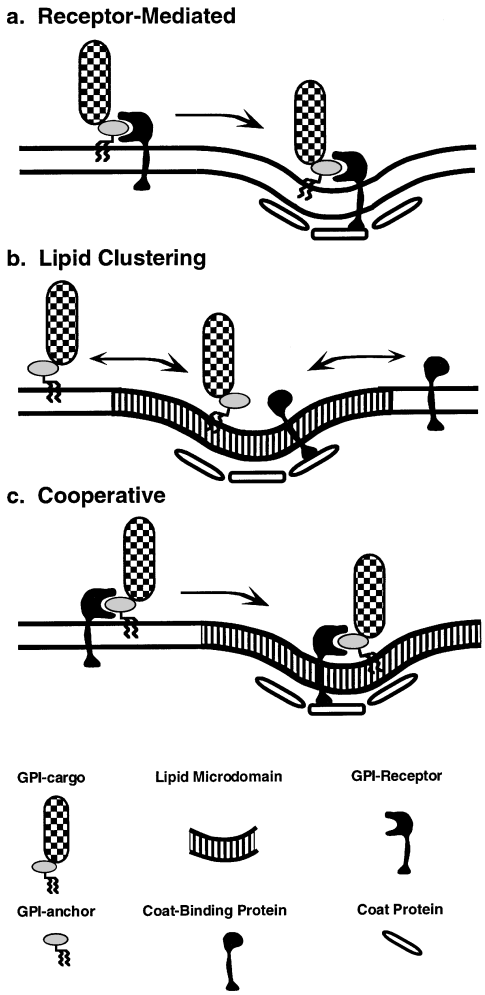

Scheme 1 Models for GPI-dependent forward transport

(**a**) Receptor-mediated model: a transmembrane receptor with a lumenal GPI-binding domain and a cytoplasmic domain capable of interacting with cytoplasmic coat proteins mediates entry of GPI-anchored cargo into budding secretory vesicles. (**b**) Lipid-clustering model: GPI-anchored cargo and transmembrane coat-binding proteins partition independently into lipid microdomains; the coat-binding protein mediates vesicle formation. (**c**) Co-operative model: the GPI-anchored cargo partitions into lipid microdomains recruiting its cognate transmembrane receptor as a complex; the cytoplasmic domain of the receptor mediates vesicle formation. In a variation of this model, the GPI receptor could also have an affinity for lipid microdomains, resulting in an enhanced partition coefficient for the complex.

One mechanism that could account for GPI-dependent secretion is that these reporters, which are normally membrane-bound, may not fold efficiently when expressed in soluble form and are consequently retained by ER molecular chaperones, e.g. BiP and calnexin, until proper assembly has been achieved (reviewed in [18]). Despite the considerable level of GPI-minus VSG in the ER, however, we find little evidence for elevated association with BiP, relative to GPI-anchored controls. Furthermore, we find that secreted mature GPI-minus VSG and, more importantly, newly synthesized VSG in the ER are both quantitatively dimerized, indicating that elimination of the GPI anchor does not impair folding and that unfolded polypeptides do not simply 'leak' into the medium. The assumption that dimerization (quaternary structure) is a valid hallmark for proper folding (tertiary structure) is implicit in this strategy, but we cannot rule out definitively the possibility that ER retention is mediated by partial localized misfolding that does not compromise dimerization. Nevertheless, we do feel that these results weigh against 'quality control' as a mechanism for regulating export of the GPI-minus reporters.

A second hypothesis maintains that the GPI anchor provides some signal or physical property that facilitates forward transport from the ER. In concordance with recent models of vesicular transport [30–32], we consider this to signify entry into budding coated secretory vesicles (note: COPI and COPII coat protein homologues have not yet been characterized in trypanosomes). Entry may be accomplished simply by concentrating GPI-anchored secretory cargo on membranes in transitional zones of the ER. If so, it may be possible to replace the GPI functionality with a peptide transmembrane domain. These experiments are in progress, but have thus far proved to be uninformative, owing to misfolding of VSG–transmembrane fusions (as judged by velocity sedimentation; results not shown).

Alternatively, the GPI moiety could be a specific ligand for a cognate receptor that mediates vesicle loading: receptor and ligand would depart together, the GPI-anchored cargo would continue along the secretory pathway and the receptor would recycle to the ER. Such a receptor would need a lumenal cargo-binding domain and a cytoplasmic domain capable of specific interaction with the cytosolic components of coated transport vesicles (Scheme 1a). Transmembrane proteins of the early secretory pathway in yeast and mammalian cells that are believed to meet these criteria include the p24 protein family [33,34] and ERGIC-53 [35,36]. Two p24 proteins, Emp24p and Erv25p, are known to play a role in transport of the major GPI-anchored protein of yeast, Gas1p [37,38]. ERGIC-53, which has a lumenal mannose-binding domain, may function in transport of secretory glycoproteins [39,40], and has recently been shown to be important for secretion of mammalian coagulation Factors V and VIII [41]. Although there is no evidence that either of these proteins interact directly with GPI structures, they do provide conceptual models for a putative GPI-specific cargo receptor.

Entry of GPI-anchored proteins into budding vesicles need not be mediated by GPI-specific receptors, however, provided that the GPI anchor confers some physical property that serves as a basis for discrimination. GPI structures are known to have an affinity for membrane lipid microdomains that are enriched with cholesterol and sphingolipids [42], and this phenomenon is believed to account for the apical routing of GPI-anchored proteins from the trans-Golgi of polarized epithelial cells [43,44]. Moreover, there is evidence that sphingolipids may play a role in exit of GPI-anchored proteins from the ER. Inhibition of ceramide synthesis, either pharmacologically [45] or by mutation [46,47], specifically lowers the rate of transport of GPI-anchored proteins in yeast; transport of non-GPI-anchored cargo, such as carboxypeptidase Y, is unaffected. On the basis of these findings, a 'lipid-clustering' model has been proposed in which GPI-anchored proteins partition into membrane microdomains in the ER, followed by the formation of GPI/sphingolipid-enriched transport vesicles [45]. However, transport of GPI-anchored proteins in yeast is dependent on COPII coat components [47], and thus requires a mechanism for mediating the assembly of a cytoplasmic coat on budding GPI-cargo vesicles. As this function cannot be directly supplied by GPI cargo, which is restricted to the lumenal leaflet of ER membranes, a clustering model may require inclusion of other transmembrane proteins to mediate vesicle formation (Scheme 1b). These proteins would associate with GPI-enriched microdomains on the basis of their own innate affinity.

These models, i.e 'receptor-mediated' versus 'lipid clustering', are not mutually exclusive and might even be 'co-operative'

(Scheme 1c). Binding to GPI-anchored cargo might actually mediate recruitment of a specific transmembrane receptor into GPI-enriched lipid microdomains, thereby providing cytoplasmic signals for efficient transport vesicle formation. In this 'co-operative' model the receptor need not have specificity for the GPI anchor, as is shown in Scheme 1(c); binding to any portion of the GPI-anchored protein would suffice. Disruption of either function, lipid clustering or specific cargo recognition, would result in impaired rates of transport, but not necessarily in a total block. This is precisely the phenotype seen in yeast with Gas1p, when ceramide synthesis is inhibited [45–47], or when Emp24p/Erv25p function is disrupted [37,38]. Other GPI-anchored molecules with no cognate cargo receptor of their own would be included in GPI transport vesicles simply by partitioning into the lipid microdomain.

In conclusion, we propose that efficient transport of GPI-anchored proteins in insect-stage trypanosomes is mediated in a positive manner by the presence of a GPI moiety. A critical test of this concept will be to accelerate the rate of transport of a reporter molecule that is not normally GPI-anchored (preferably of non-trypanosomal origin) by addition of a GPI-peptide sequence. Another important issue that must also be addressed is the generality of GPI-dependent transport. These findings must be extended not only to bloodstream trypanosomes, but also to other eukaryotic organisms. GPI-anchored proteins exist in most (probably all) eukaryotes, but protozoa are extreme in their use of this mode of membrane attachment, e.g. VSG comprises $\approx 10\,\%$ of total cell protein in bloodstream trypanosomes. As a result of the need to efficiently transport such large amounts of surface proteins, protists may have fine-tuned GPI-dependent transport mechanisms to the point of 'over-reliance'. However, if this phenomenon proves to be common to other eukaryotes, our findings may lay the groundwork for a generalized concept of GPI function in eukaryotic secretory trafficking.

We are indebted to Dr. Dan Eichinger, Dr. David Engman, Dr. Ian Manger and Dr. Sergio Schenkman for providing reagents. We are grateful to Dr. Tamara Doering, Dr. Sebastian Bednarek, Dr. Anant Menon and Dr. Jolanta Vidugiriene for thoughtful discussions and a critical reading of the manuscript. We also acknowledge the constant inspiration of Samuel Ferdig. This work was supported in part by National Institutes of Health Grant AI35739. M.A.M. was supported by National Institutes of Health Cellular and Molecular Parasitology Training Grant AI07414. J.D.B. is a recipient of a Burroughs Wellcome Fund New Investigator Award in Molecular Parasitology.

REFERENCES

1 Ferguson, M. A. J., Homans, S. W., Dwek, R. A. and Rademacher, T. W. (1988) Science **239**, 753–759
2 Low, M. G. and Kincade, P. W. (1985) Nature (London) **318**, 62–64
3 Tse, A. G. D., Barclay, A. N., Watts, A. and Williams, A. F. (1985) Science **230**, 1003–1008
4 Takami, N., Ogata, S., Oda, K., Misumi, Y. and Ikehara, Y. (1988) J. Biol. Chem. **263**, 3016–3021
5 Englund, P. T. (1993) Annu. Rev. Biochem. **62**, 121–138
6 Udenfriend, S. and Kodukula, K. (1995) Annu. Rev. Biochem. **64**, 563–591
7 Lisanti, M. and Rodriguez-Boulan, E. (1990) Trends Biochem. Sci. **15**, 113–118
8 Lisanti, M., Carase, I. P., Davitz, M. A. and Rodriguez-Boulan, E. (1989) J. Cell Biol. **109**, 2145–2156
9 Brown, D. A., Crise, B. and Rose, J. K. (1989) Science **245**, 1499–1251
10 Conzelmann, A., Spiazzi, A., Bron, C. and Hyman, R. (1988) Mol. Cell. Biol. **8**, 674–678
11 Moran, P. and Caras, I. W. (1992) J. Cell Biol. **119**, 763–772
12 Field, M. C., Moran, P., Li, W., Keller, G. A. and Caras, I. W. (1994) J. Biol. Chem. **269**, 10830–10837
13 Doering, T. L. and Schekman, R. (1996) EMBO J. **15**, 182–191
14 Bernasconi, E., Fasel, N. and Wittek, R. (1996) J. Cell Sci. **109**, 1195–1201
15 Bangs, J. D., Ransom, D. M., McDowell, M. A. and Brouch, E. M. (1997) EMBO J. **16**, 4285–4294
16 Cross, G. A. M. (1975) Parasitology **71**, 393–417
17 Stebeck, C. and Pearson, T. W. (1994) Exp. Parasitol. **78**, 432–436
18 Hammond, C. and Helenius, A. (1995) Curr. Opin. Cell Biol. **7**, 523–529
19 Bangs, J. D., Brouch, E. M., Ransom, D. M. and Roggy, J. L. (1996) J. Biol. Chem. **271**, 18387–18393
20 Harlow, E. and Lane, D. (1988) Antibodies: A Laboratory Manual, Cold Spring Harbor Laboratory, Cold Spring Harbor, NY
21 Bangs, J. D., Uyetake, L., Brickman, M. J., Balber, A. E. and Boothroyd, J. C. (1993) J. Cell Sci. **105**, 1101–1113
22 Uemura, H., Schenckman, S., Nussenzweig, V. and Eichinger, D. (1992) EMBO J. **11**, 3837–3844
23 Kolodziej, P. A. and Young, R. A. (1991) Methods Enzymol. **194**, 508–519
24 Mowatt, M. R. and Clayton, C. E. (1987) Mol. Cell. Biol. **7**, 2833–2844
25 Delahunty, M. D., Stafford, F. J., Yuan, L. C., Shaz, D. and Bonifacino, J. S. (1993) J. Biol. Chem. **268**, 12017–12027
26 Nuoffer, C., Horvath, A. and Riezman, H. (1993) J. Biol. Chem. **268**, 10558–10563
27 Garg, N., Tarleton, R. L. and Mensa-Wilmot, K. (1997) J. Biol. Chem. **272**, 12482–12491
28 Nuoffer, C., Jeno, P., Conzelmann, A. and Riezman, H. (1991) Mol. Cell. Biol. **11**, 27–37
29 Pauly, P. C. and Klein, C. (1995) Biochem. J. **306**, 643–650
30 Schekman, R. and Orci, L. (1996) Science **271**, 1526–1533
31 Rothman, J. E. and Wieland, F. T. (1996) Science **272**, 227–234
32 Bednarek, S. Y., Orci, L. and Schekman, R. (1996) Trends Cell Biol. **6**, 468–473
33 Stamnes, M. A., Craighead, M. W., Hoe, M. E., Lampen, N., Geromanos, S., Tempst, P. and Rothman, J. E. (1995) Proc. Natl. Acad. Sci. U.S.A. **92**, 8011–8015
34 Fiedler, K., Veit, M., Stamnes, M. A. and Rothman, J. E. (1996) Science **273**, 1396–1399
35 Schindler, R., Itin, C., Zerial, M., Lottspeich, F. and Hauri, H. P. (1993) Eur. J. Cell Biol. **61**, 1–9
36 Kappeler, F., Klopfenstein, D. R. C., Foguet, M., Paccaud, J.-P. and Hauri, H.-P. (1997) J. Biol. Chem. **272**, 31801–31808
37 Schimmoller, F., Singer-Kruger, B., Schroder, S., Kruger, U., Barlowe, C. and Riezman, H. (1995) EMBO J. **14**, 1329–1339
38 Belden, W. J. and Barlowe, C. (1996) J. Biol. Chem. **271**, 26939–26946
39 Arar, C., Carpentier, V., Le Caer, J. P., Monsigny, M., Legrand, A. and Roche, A. C. (1995) J. Biol. Chem. **270**, 3551–3553
40 Itin, C., Roche, A. C., Monsigny, M. and Hauri, H. P. (1996) Mol. Cell. Biol. **7**, 483–493
41 Nichols, W. C., Seligsohn, U., Zevilin, A., Terry, V. H., Hertel, C. E., Wheatley, M. A., Moussalli, M. J., Hauri, H.-P., Ciavarella, B., Kaufman, R. J. and Ginsburg, D. (1998) Cell **93**, 61–70
42 Harder, T. and Simons, K. (1997) Curr. Opin. Cell Biol. **9**, 534–542
43 Brown, D. A. and Rose, J. K. (1992) Cell **68**, 533–544
44 Zurzolo, C., van't Hof, W., van Meer, G. and Rodriquez-Boulan, E. (1994) EMBO J. **13**, 42–53
45 Horvath, A., Sutterlin, C., Manning-Krieg, U., Roa Movva, N. and Riezman, H. (1994) EMBO J. **13**, 3687–3695
46 Skrzypek, M., Lester, R. L. and Dickson, R. C. (1997) J. Bacteriol. **179**, 1513–1520
47 Sutterlin, C., Doering, T., Schimmoller, F., Schroder, S. and Riezman, H. (1997) J. Cell Sci. **110**, 2703–2714
48 Boothroyd, J. C., Paynter, C. A., Cross, G. A. M., Bernards, A. and Borst, P. (1981) Nucleic Acids Res. **9**, 4735–4743

Received 22 June 1998/22 July 1998; accepted 24 August 1998